Published in final edited form as:
J Control Release. 2007 November 6; 123(2): 141–147.

Tracking the Dephosphorylation of Resveratrol Triphosphate in Skin by Confocal Raman Microscopy

Guojin Zhang, **Carol R. Flach**[§], and **Richard Mendelsohn**
Department of Chemistry, Newark College of Arts and Sciences, Rutgers University, Newark, New Jersey, 07102, USA

Abstract

Polyphenolic resveratrol has been identified as a potent antioxidant acting as both a free radical scavenger and an inhibitor of enzyme oxidative activity. However, the reactive propensity of resveratrol also limits its use in topical formulations. A transient derivative of resveratrol, resveratrol triphosphate, has been designed to provide a means for the delayed delivery of the active compound in skin tissue where endogenous enzymes capable of dephosphorylation reside. Confocal Raman microscopy studies of intact pigskin biopsies treated with modified resveratrol provided information about the spatial distribution and time-dependence of permeation and conversion to the native active form. Conversion to the active form was not observed when skin samples were exposed to steam, a procedure that likely inactivates endogenous skin enzymes. In addition, treatment with the triphosphate compared to the parent compound revealed a more homogeneous distribution of resveratrol throughout the stratum corneum and viable epidermis when the former was applied. Thus, the bioavailability of resveratrol in the epidermis appears to be enhanced upon application of the pro-molecule compared to resveratrol.

Keywords

confocal Raman spectroscopy; resveratrol; permeation; prodrug; epidermis

INTRODUCTION

Resveratrol (*trans*-3,4′,5-trihydroxystilbene) is one of several biologically active polyphenolic compounds found in a wide variety of plant species, which are well known for their antioxidant properties. The antioxidant activities of polyphenols are based on the ease with which the hydrogen of the phenolic compounds can be donated to neutralize free radicals produced by oxidative processes such as phospholipid peroxidation via UV radiation or by biologically mediated events. It has been demonstrated that resveratrol may serve both as a primary antioxidant (free radical scavenger), which can directly react with free radicals and convert them into products [1–3], and as a secondary (preventive) antioxidant, which can lower the rate of oxidation by inhibiting enzyme activities. For example, resveratrol has been shown to inhibit the activities of cyclooxygenase, lipooxygenase, and xanthine oxidase where increased levels of these enzymes lead to a variety of diseases [2,4]. Beneficial effects of resveratrol on neurological, hepatic, and cardiovascular systems have been extensively explored [5,6]. More

[§]Corresponding author: Tel.:973-353-1330; Fax: 973-353-1264; e-mail: flach@andromeda.rutgers.edu.

recently, resveratrol has been identified as a potential cancer-chemopreventive agent, blocking the multi-step process of carcinogenesis at various stages [4,7,8].

Human skin is frequently exposed to oxidative stress; subsequent damage is likely an important factor in the pathogenesis of skin cancer and photoaging. Resveratrol has been widely used in pharmaceutical and cosmetic formulations as an antioxidant and a chemopreventive agent. However, due to its free radical scavenger properties, resveratrol itself becomes susceptible to external reactive oxygen species. Thus, the efficacy of resveratrol is decreased upon exposure to heat and light resulting in diminished bioavailability.

Various methods have been developed to increase the bioavailability of topically applied active agents, for example, the use of permeation enhancers in combination with microemulsions, polymeric solutions, or prodrugs [9–12]. In one study, a biodegradable enhancer was designed to take advantage of the barrier recovery properties of its metabolite, tranexamic acid [13]. In the current study, a prodrug approach is employed. The three hydroxyl groups of resveratrol have been phosphorylated (Fig. 1) to reduce the susceptibility to degradation and thus to provide better stability [14]. Modified resveratrol is expected to be dephosphorylated to the native, active form either chemically or by enzymes existing in tissues. It is well known that the epidermis contains many enzymes, such as proteases, esterases, lipases, and phosphatases [15–17]. Reports of the metabolism of several topically applied prodrugs, including pro-vitamins, to their active forms in human skin and skin models have been recently published [18–20]. Thus, phosphorylated resveratrol may be particularly effective in topical formulations applied to skin

In general, traditional methods of evaluating permeation and metabolism of exogenous material topically applied to skin either perturb skin structure or expose skin to non-physiological conditions. One common method involves the use of a Franz diffusion cell, in which a buffer solution is in constant contact with the dermis (acceptor phase) possibly extracting skin constituents and changing the physiological state of skin. Subsequent HPLC and mass spectroscopy of the acceptor phase to identify and quantify permeants provides high selectivity and sensitivity; however, information pertaining to the spatial distribution of the exogenous substances in skin and possible perturbations to the structure of endogenous skin components is lacking. Tape stripping the uppermost cornified layers of skin, the stratum corneum (SC), is another common protocol. Depth dependent concentration profiles and an evaluation of endogenous skin structure can be obtained when tape stripping is followed with a technique such as attenuated total reflection infrared spectroscopy (ATR-IR) or extraction followed by HPLC. One study of human epidermis found that the flux data for the permeation of increasing concentrations of a lipophilic model drug from Franz diffusion cell experiments were linearly related to the steady state drug amount in the SC determined by HPLC after extraction from tape strips [21]. It is evident that the aforementioned approaches provide predictive measures of permeation and penetration; however, the sampling is limited to the SC under conditions where tape stripping is applied and spatial heterogeneity in the plane parallel to the skin surface cannot be determined.

The applicability of confocal Raman microscopy as a non-invasive optical approach for studies of the delivery and metabolism of prodrug and drugs has been previously demonstrated [20]. The unique advantage of this technique is its capability to provide direct spatially resolved concentration and molecular structure information while keeping the sample intact under essentially *in vivo* conditions. By optically dissecting the skin with a spatial resolution of 1 μm in the x and y directions (parallel to the skin surface) and 2–3 μm in the z direction (depth in skin), the delivery and metabolism of exogenous material related to skin heterogeneity are presented in detail. Previous studies also demonstrated the feasibility of utilizing confocal Raman for the *in situ* examination of biochemical heterogeneity at a single cellular level [22].

In the current study, this novel approach is applied to track the permeation and hydrolysis of resveratrol triphosphate in skin.

MATERIALS AND METHODS

Materials

Resveratrol was purchased from Sigma-Aldrich Chemical Co. (St Louis, MO). Resveratrol triphosphate trisodium was generously provided by Omni-Chem (Louvain-la-Neuve, Belgium). Wickenol 161 was provided by ALZO International Incorp. (Sayreville, NJ). Skin biopsies from Yucatan white, hairless pigs were purchased from Sinclair Research Center, Inc. (Columbia, MO).

Sample preparation

The Rutgers University Internal Review Board has approved all protocols used herein. Raman spectra were acquired from resveratrol in ethanol (0.2M) and resveratrol triphosphate trisodium in water (0.2M). Separate suspensions of resveratrol triphosphate and resveratrol in Wickenol 161 were prepared by stirring mixtures (~0.2M) for 48h at room temperature. Each suspension has enough excess solid to maintain saturation. Suspensions were topically applied to the stratum corneum of intact pigskin at a surface coverage of 5μl/cm^2. Samples were sealed to prevent dehydration and held at 34°C for 20h after which excess solid remaining on the surface was rinsed off using fresh Wickenol 161. The treated skin samples were gently pressed, stratum corneum side up into a milled brass cell, covered with a microscope coverslip, and sealed for confocal Raman measurements.

For particular experiments, pigskin samples were steamed prior to the application of exogenous material. The procedure was conducted using a diffusion cell. A skin section of full thickness (including dermis) was clamped in the cell with the SC facing the lower compartment. Water in the lower compartment was brought to boiling. The surface of the SC was exposed to steam for ~10 min. A resveratrol triphosphate suspension was then applied to the skin section following the above protocol.

Another set of experiments used skin sections where the SC was removed by tape stripping. Several small Raman maps were acquired of the tape-stripped skin surface after each set of ~10 tapes to determined if the SC was completely removed. Several Raman spectral signatures allow for the discrimination of the SC from the underlying, viable epidermis [23]. A total of ~35 tape strips provided complete removal of the SC. Subsequently, a suspension of resveratrol triphosphate was applied following the above protocol.

Confocal Raman microspectroscopy

Raman spectra were acquired with a Kaiser Optical Systems Raman Microprobe (Ann Arbor, MI). The instrument has been previously described in detail [23]. Briefly, excitation is achieved with a solid-state diode laser at 785nm. Approximately 8–12mW of single mode power is focused with a 100x oil immersion objective to a volume of ~2μm^3 within the sample. A drop of oil is placed on top of a microscope coverslip which is in contact with the underlying skin sample. The backscattered light illuminates a near-IR CCD (ANDOR Technology, Model DU 401-BR-DD) with spectral coverage over 100-3450 cm^{-1} at a spectral resolution of 4 cm^{-1}. Data are encoded every 0.3 cm^{-1} following linearization. Spectra are acquired using a 60s exposure time, 4 accumulations, and cosmic ray correction. Confocal maps (axial lines and planes) were obtained at room temperature perpendicular to the skin surface using a step size of 3μm. The time required to acquire an image plane varies with size and spatial resolution. Previously published protocols [23,24] were used to evaluate axial characteristics of the current optical set-up. Briefly, the use of the oil immersion lens provides better refractive index

matching with the skin sample than a dry objective, lessening depth distortion (to ~10%) and maximizing laser power. The actual axial spatial resolution in the skin samples cannot be directly ascertained but is estimated at ~2 μm.

Data analysis

Grams/32 AI software version 6.0 (ThermoGalactic, Salem, NH) was used for linear baseline correction of the individual Raman spectra of solutions. ISys software version 3.1 (Malvern Instruments, Inc., Southborough, MA) was used for all other data processing (linear baseline correction, determination of peak position, band area integration) and to generate Raman image planes. The Spectral Moments function in ISys uses a conventional center of gravity algorithm to determine band position. Spectral regions used for data processing are specified in figure captions.

RESULTS AND DISCUSSION

A Raman spectrum of untreated pigskin acquired at a depth of ~6μm beneath the stratum corneum surface along with spectra of resveratrol and resveratrol triphosphate (R-P_3) solutions in the 600–1700 cm^{-1} region are presented in Fig. 2a, c, and d, respectively. A spectrum of Wickenol 161, commonly used in personal care products as an emollient and used in the current experiments as a delivery agent for R-P_3, is also included in Fig. 2b. The spectrum of pigskin displays several bands characteristic of the lipid and protein constituents of the SC, e.g. the phe ring breathing mode at 1004 cm^{-1} and the Amide I band at ~1650 cm^{-1}, predominantly due to the helical structure of keratin. The structural similarity of resveratrol and R-P_3 is reflected in the resemblance of the spectral features shown in Fig. 2c and d, respectively. Ideally, discrete bands resolved from those observed for skin and the delivery agent would be diagnostic for the presence of each molecule in skin. It is evident from the figure that the dominant bands in spectrum of Wickenol 161 do not interfere with those of resveratrol or R-P_3. Raman spectra of resveratrol and R-P_3 solutions highlighting the spectral regions used in subsequent analyses are shown in Fig. 3a. In the following examination, the band observed at 995 cm^{-1} in the spectrum of resveratrol and the position of maximum intensity in the overlapped 1600/1610 cm^{-1} pair observed in R-P_3 and resveratrol (see Fig. 3a), serve to track the permeation and conversion of resveratrol triphosphate to resveratrol in skin. Bands in the 1000 cm^{-1} region are due to the aromatic ring breathing mode while those in the low 1600 cm^{-1} region arise from conjugated C=C double bond and ring stretching modes.

A suspension of 0.2M resveratrol triphosphate in Wickenol 161 was topically applied to pigskin for 20h at 34°C. Subsequently, a series of confocal Raman spectra from treated skin were acquired every 3μm to an overall depth of 60μm. The first 10 spectra in two regions of interest, 920–1014 cm^{-1} and 1560–1700 cm^{-1}, are shown in Fig. 3b. Spectral features arising from both skin (phe at 1004 cm^{-1}) and the exogenous resveratrol compounds are evident in the data. The 995 cm^{-1} band indicative of resveratrol is observed as a shoulder on the low frequency side of the phe band. The presence of the band in skin indicates that resveratrol triphosphate dephosphorylation has taken place in the top layers of the skin, i.e., the stratum corneum. It is of interest to note that the position of the phe band only in the outermost layer sampled (top spectrum in left hand side of Fig. 3b) is slightly shifted to lower wavenumbers most likely due to a contribution from the 1001 cm^{-1} band of R-P_3. In the second spectrum in the series, acquired at a depth of ~6 μm under the skin surface, the phe band is observed at its normal position, i.e. at the same wavenumber position (1004 cm^{-1}) as in untreated skin. The spectra of treated skin shown in the 1560–1700 cm^{-1} region (Fig. 3b) corroborate that dephosphorylation has taken place. The band at 1605 cm^{-1} displayed in the first spectrum of Fig. 3b most likely arises from a mixture of resveratrol and of mono-, di- and triphosphorylated resveratrol compounds. Deeper in skin, this band shifts to higher wavenumbers (~1607

cm^{-1}), indicative of further R-P_3 dephosphorylation. A sequence of intermediates likely forms as dephosphorylation proceeds in skin. In a related control experiment, confocal Raman spectra were acquired after a suspension of resveratrol in Wickenol 161 was applied to skin using the same experimental conditions. In these spectra, the C=C stretching mode was observed in the 1606–1610 cm^{-1} range supporting the use of band positions to qualitatively measure the extent of dephosphorylation.

It is of interest to consider whether R-P_3 dephosphorylation in skin occurs enzymatically or through non-specific chemical hydrolysis. A control experiment was conducted to determine the stability of the triphosphate molecule where R-P_3 was incubated for 60h at 34°C in a buffer solution at pH 5.5, close to the pH and temperature reported for the stratum corneum [25]. Resveratrol bands were not detected in the Raman spectrum of this solution (not shown) demonstrating the chemical stability of R-P_3. To investigate endogenous enzyme activity, the SC of an intact pigskin sample was exposed to steam for 10 minutes prior to the application of the R-P_3 suspension. In an earlier report, the activities of SC enzymes responsible for ester hydrolysis were shown to be heat labile [26]. The enzymes responsible for dephosphorylation in the current experiments also appear to be heat labile. Twenty lines of confocal Raman spectra were acquired from the heat-treated skin sample. A representative series of Raman spectra from one confocal line are presented in Fig. 3c. While the presence of the bands in the 1600 cm^{-1} region indicate that permeation to at least 30 μm in skin has taken place, the absence of the 995 cm^{-1} resveratrol band is strong evidence that dephosphorylation has not occurred. This interpretation is supported by the position of the C=C stretching band (~1600 cm^{-1}) in spectra acquired from the outermost SC layers which is similar to that of the R-P_3 solution (compare right hand side of Fig. 3a with c). Variations in the C=C band position and width are observed with depth in Fig. 3c. The nature of the change is non-monotonic and may reflect simply experimental noise or areas where enzymes were not affected by the heat-treatment. Another possibility is that other metabolic products may have formed. It is of interest to note that the Amide I band position is affected by the steaming process (compare right hand side of Fig. 3c with 3b and 2a). A shift in frequency from ~1650 to ~1667 cm^{-1} reflects a change in protein (mostly keratin) secondary structure from predominantly helical to β-sheet and most likely indicates that thermal denaturation of protein has taken place. It is thus also possible that the skin enzymes have denatured, disrupting binding sites and disabling their ability to function. This result strongly supports the enzymatic dephosphorylation of resveratrol triphosphate to resveratrol in skin. It is well known that a variety of skin enzymes exist in stratum corneum to maintain skin barrier function [26–28].

To evaluate the temporal and spatial variation of dephosphorylation in skin, confocal Raman images were acquired of different skin regions, i.e., stratum corneum and viable epidermis, at increasing times after exposure to R-P_3 suspensions. More specifically, it is of interest to ascertain whether dephosphorylation takes place only in stratum corneum or also in the viable epidermis and to explore the time dependence of this process. In the first set of experiments, a 0.2 M resveratrol triphosphate suspension was applied to the intact skin surface for 5h at 34° C. The acquisition of Raman spectra over the same area, encompassing the SC (top of the image shown in Fig. 4a) and the boundary to underlying epidermis, was initiated after 7, 22, and 33h. Image planes of the C=C stretching band frequency, increasing in time from left to right, are shown in Fig. 4a (i–iii). Signal to noise levels in the Raman spectra for the C=C band decrease with depth from ~50/1 to 20/1. It has been shown that band position can be obtained at high precision (thus a frequency error of $\leq$0.04 cm^{-1} is feasible for a S/N of 20/1) using the topmost $\geq$60% of the band and a center of gravity algorithm [29]. In the current analysis, at least 90% of the band area is used to yield a precise measure of peak position. Thus, the results provide a measure of the relative formation of resveratrol from R-P_3. As the position of the C=C band shifts to higher wavenumbers (red), the amount of resveratrol in the SC increases relative to R-P_3. In the time-resolved frequency image planes shown in Fig. 4a, an increase in frequency

is displayed from left to right demonstrating that dephosphorylation of resveratrol triphosphate proceeds in a time-dependent fashion. The relatively larger concentration of resveratrol in the deeper regions of the SC may be due to both dephosphorylation taking place at this depth and permeation of resveratrol (that was dephosphorylated in the outermost layers) with time. More sensitive methods of detection are needed to "uncouple" diffusion from kinetics of hydrolysis.

To explore dephosphorylation in the viable epidermis, the stratum corneum was removed by tape stripping prior to the application of the resveratrol triphosphate suspension. A dose of 0.2M R-P_3 was applied to the epidermis for 20h at 34°C. Raman spectra were acquired over an area of 70μm (depth) × 30μm (width). An image plane of the C=C band position is shown in Fig. 4b where data collection began with the acquisition of the confocal line of spectra on the left side of the image and proceeded from left to right (total of 8 lines of spectra) with each "z-line" requiring ~100 min. Total acquisition time was ~13h. The frequency map shown in Fig. 4b depicts an increase in the relative concentration of resveratrol with time, however, the range of the frequency increase is less than half that of the range shown for the application to the SC (Fig. 4a) where the acquisition of each "z-line" required ~ 40 min. A comparison of the frequency image planes generated from the two different epidermal regions clearly indicate that the extent and rate of dephosphorylation in the viable epidermis is significantly less than in the SC. This finding may have important ramifications with regard to resveratrol's bioavailability and efficacy as an antioxidant.

A comparison of the spatial distribution of resveratrol in the SC and underlying epidermis resulting from the application of R-P_3 versus resveratrol provides further insight into resveratrol bioavailability. In separate experiments, a 0.2M suspension of either resveratrol or R-P_3 was applied to the SC of intact pigskin for 20hrs at 34°C. Raman image planes of the same size, 60μm (depth) × 24μm (width), were then acquired from the two pieces of skin. An evaluation of relative resveratrol concentration in skin was conducted as follows. The phe ring breathing mode at 1004 cm^{-1}, mainly arising from endogenous skin proteins, serves as an internal standard for Raman intensity. As discussed in a previous report, this band calibrates for confocal scattering losses with depth in the skin [20]. Since there is some overlap between the resveratrol band at 995 cm^{-1} and phe band at 1004 cm^{-1} (Fig. 5a), the band area ratio of the low frequency half of the 995 cm^{-1} band ratioed to the high frequency half of the phe band (shaded in Fig. 5a) was used to characterize the relative concentration of resveratrol in skin. Area ratio maps for both experiments are shown in Fig. 5b. It is noted that the band at 1001 cm^{-1} from resveratrol triphosphate may potentially interfere with the analysis (Fig 3a and b); however, the extent of the perturbation is lessened by integrating the high frequency half of the phe band and may be negligible due to the relatively rapid rate of dephosphorylation in the SC as described above. As Fig. 5b illustrates, there are obvious differences in the distribution of resveratrol in skin depending on which molecule is applied. As may be expected, a higher concentration of resveratrol is observed in the SC when a suspension of resveratrol compared to R-P_3 is applied (compare the top 15–20 μm in Fig. 5b, ii vs. i, respectively). Furthermore, the delineation between the SC and viable epidermis is more clearly visible in the image on the right (resveratrol application) compared to the more gradual decrease in relative resveratrol concentration observed when the phosphorylated molecule is applied (image on left). In an earlier report from this laboratory, the thickness of the SC for similar untreated pigskin biopsies was shown to be ~15–20 μm [20]. This thickness is consistent with the region depicting a relatively high resveratrol concentration as shown in Fig. 5b (ii). The significant decrease in relative resveratrol concentration at the SC/viable epidermal boundary when resveratrol, as opposed to R-P_3, is applied is suggested to be due to the increased water content of the viable epidermis (compared to the SC) and the insolubility of resveratrol in water. In contrast, it is the higher water content in the viable epidermis that facilitates the permeation of water soluble R-P_3 into this region. As was shown above (Fig. b), dephosphorylation also takes place in the

viable epidermis creating a more homogenous distribution of resveratrol and hence greater bioavailability in this region when R-P_3 is applied.

The current investigation demonstrates the ability of confocal Raman microscopic imaging to monitor the time course and spatial distribution of exogenous agent permeation and metabolism with respect to skin microanatomy (to depths of ~70 μm). The inherent strength of the techniques utilized herein and in previous studies [13] allows for the discrimination of closely related chemical species and physical states in tissue. It is easy to envision applications that evaluate a series of pro-molecules including their conversion to active forms for use in both pharmaceutical and cosmetic industries.

Acknowledgements

This work was supported by PHS Grant GM 29864 to R.M.

References

1. Fauconneau B, Waffo-Teguo P, Huguet F, Barrier L, Decendit A, Merillon JM. Comparative study of radical scavenger and antioxidant properties of phenolic compound from *vitis vinifera* cell cultures using *in vitro* tests. Life Sci 1997;61:2103–2110. [PubMed: 9395251]
2. Acquaviva R, Russo A, Campisi A, Sorrenti V. Antioxidant activity and protective effect on DNA cleavage of resveratrol. J Food Technol 2002;67:137–141.
3. Li ZD, Ma QY, Wang CA. Effect of resveratrol on pancreatic oxygen free radicals in rats with severe acute pancreatitis. World J Gastroentero 2006;12:137–140.
4. Bhat PLK, Pezzuto JM. Cancer chemopreventive activity of resveratrol. Ann NY Acad Sci 2002;957:210–229. [PubMed: 12074974]
5. Baur JA, Sinclair DA. Therapeutic potential of resveratrol: the *in vivo* evidence. Nat Rev Drug Discov 2006;5:493–506. [PubMed: 16732220]
6. Bradamante S, Barenghi L, Villa A. Cardiovascular protective effects of resveratrol. Cardiovasc Drug Rev 2004;22:169–188. [PubMed: 15492766]
7. Jang M, Cai L, Udeani GO, Slowing KV, Thomas CF, Beecher CWW, Fong HHS, Farnsworth NR, Kinghorn AD, Mehta RG, Moon RC, Pezzuto JM. Cancer chemopreventative activity of resveratrol, a natural product derived from grapes. Science 1997;275:218–220. [PubMed: 8985016]
8. Sengottuvelan M, Viswanathan P, Nalini N. Chemopreventive effect of trans-resveratrol - a phytoalexin against colonic aberrant crypt foci and cell proliferation in 1,2-dimethylhydrazin incuded colon carcinogenesis. Carcinogenesis 2006;27:1038–1046. [PubMed: 16338953]
9. Williams AC, Barry BW. Penetration enhancers. Adv Drug Deliv Rev 2004;56:603–618. [PubMed: 15019749]
10. Sintov AC, Shapiro L. New microemulsion vehicle facilitates percutaneous penetration in vitro and cutaneous drug bioavailablity in vivo. J Control Release 2004;95:173–183. [PubMed: 14980766]
11. Sloan KB, Wasdo SC, Rautio J. Design for optimized topical delivery: Prodrugs and a paradigm change. Pharm Res 2006;23:2729–2747. [PubMed: 17109215]
12. Schroeder IZ, Franke P, Schaefer UF, Lehr CM. Delivery of ethinylestradiol from film forming polymeric solutions across human epidermis in vitro and in vivo in pigs. J Control Release 2007;118:196–203. [PubMed: 17289207]
13. Vávrová D, Hrabálek A, Doležal P, Holas T, Klimentová J. Biodegradable derivatives of tranexamic acid as transdermal acid as transdermal permeation enhancers. J Control Release 2005;104:41–49. [PubMed: 15866333]
14. DeClercq, L.; Corstjens, H.; Maes, D.; Van Brussel, W.; Schelkens, G. Topical compositions containing phsophorylated polyphenols, World Intellectual Property Organization WO 2006/029484; 23 March 2006;
15. Prusakiewicz JJ, Ackermann C, Voorman R. Comparison of skin esterase activities from different species. Pharm Res 2006;23:1517–1524. [PubMed: 16779705]

16. Redoules D, Perie JJ, Viode C, Mavon A, Fournier D, Daunes S, Casas C, Lougarre A, De Viguerie N. Slow internal release of bioactive compounds under the effect of skin enzymes. J Invest Dermatol 2005;125:270–277. [PubMed: 16098037]

17. Amr S, Brown MB, Martin GP, Forbes B. Activation of clindamycin phosphate by human skin. J Appl Microbiol 2001;90:550–554. [PubMed: 11309066]

18. Ostacolo C, Marra F, Laneri S, Sacchi A, Nicoli S, Padula C, Santi P. α-tocopherol pro-vitamins: synthesis, hydrolysis and accumulation in rabbit ear skin. J Control Release 2004;99:403–413. [PubMed: 15451598]

19. Mavon A, Raufast V, Redoules D. Skin absorption and metabolism of a new vitamin E prodrug, δ-tocopherol-glucoside: in vitro evaluation in human skin models. J Control Release 2004;100:221–231. [PubMed: 15544870]

20. Zhang G, Moore DJ, Sloan KB, Flach CR, Mendelsohn R. Imaging the prodrug-to-drug transformation of a 5-Fluorouracil derivative in skin by confocal Raman microscopy. J Inves Derm 2007;127:1205–1209.

21. Wagner H, Kostka KH, Lehr CM, Schaefer UF. Interrelation of permeation and penetration parameters obtained from in vitro experiments with human skin and skin equivalents. J Control Release 2001;75:283–295. [PubMed: 11489316]

22. Zhang G, Moore DJ, Mendelsohn R, Flach CR. Vibrational microspectroscopy and imaging of molecular composition and structure during human corneocyte maturation. J Invest Dermatol 2006;126:1088–1094. [PubMed: 16514411]

23. Zhang G, Moore DJ, Flach CR, Mendelsohn R. Vibrational microscopy and imaging of skin: from single cells to intact tissue. Anal Bioanal Chem 2007;387:1591–1599. [PubMed: 17160382]

24. Xiao C, Flach CR, Marcott M, Mendelsohn R. Uncertainties in depth determination and comparison of multivariate with univariate analysis in confocal Raman studies of a laminated polymer and skin. Appl Spectrosc 2004;58:382–389. [PubMed: 15104806]

25. Kraning, KK. Physiology, Biochemistry, and Molecular Biology of the Skin. Goldsmith, LA., editor. Oxford University Press; New York: 1991. p. 1085-1095.

26. Beisson F, Aoubala M, Marull S, Moustacas-Gardies A, Voultoury R, Verger R, Arondel V. Use of the tape stripping technique for directly quantifying esterase activities in human stratum corneum. Anal Biochem 2001;290:179–185. [PubMed: 11237319]

27. Sugibayashi K, Hayashi T, Morimoto Y. Simultaneous transport and metabolism of ethyl nicotinate in hairless rat skin after its topical application: the effect of enzyme distribution in skin. J Control Release 1999;62:201–208. [PubMed: 10518652]

28. Harding CR. The stratum corneum: structure and function in health and disease. Dermatol Ther 2004;17:6–15. [PubMed: 14728694]

29. Cameron DG, Kauppinen JK, Moffatt DJ, Mantsch HH. Precision in condensed phase vibrational spectroscopy. Appl Spectrosc 1982;36:245–250.

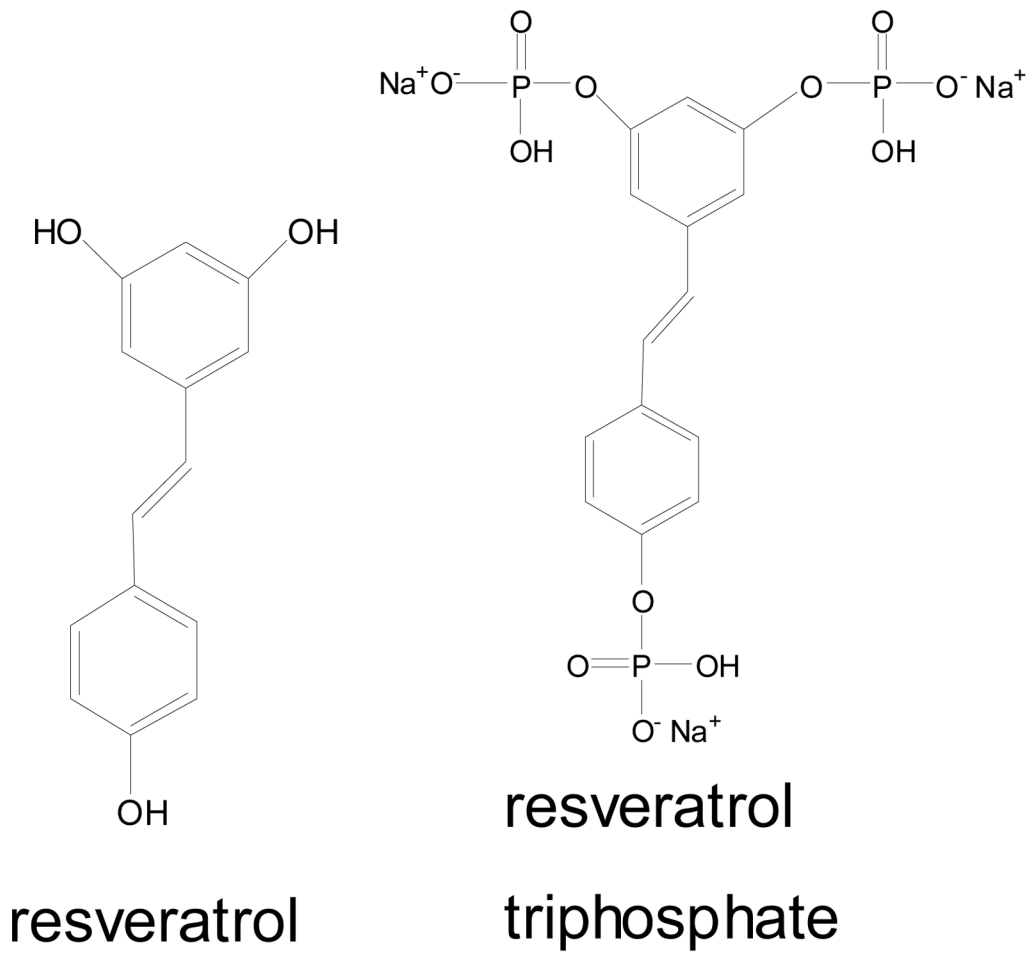

Fig. 1.
Chemical structures of resveratrol and resveratrol triphosphate trisodium (R-P_3).

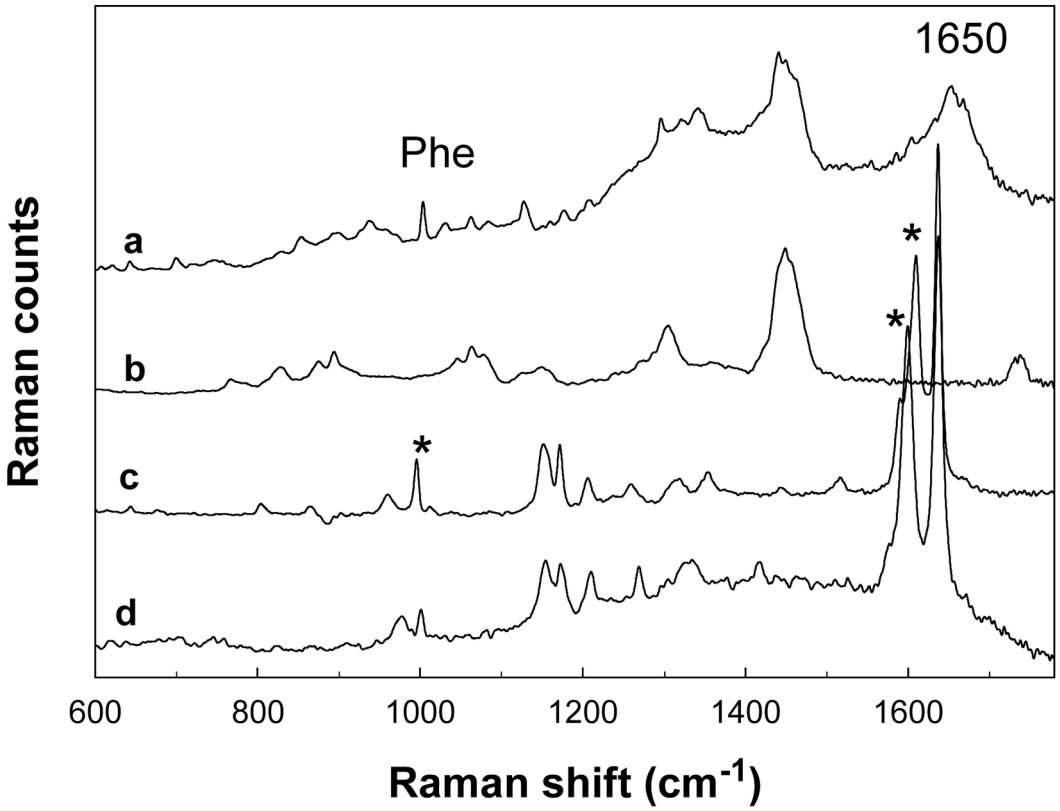

Fig. 2.

Raman spectra (600–1700 cm^{-1}) depicting diagnostic bands for resveratrol and resveratrol triphosphate permeation and metabolism in skin: (a) confocal Raman spectrum of untreated pigskin acquired at a depth of ~6 μm below the skin surface, (b) spectrum of neat Wickenol 161, (c) spectrum of a 0.2 mM resveratrol solution in ethanol after ethanol subtraction, (d) spectrum of an aqueous solution of resveratrol triphosphate. The asterisks mark the main diagnostic bands for tracking resveratrol and resveratrol triphosphate used in the current study.

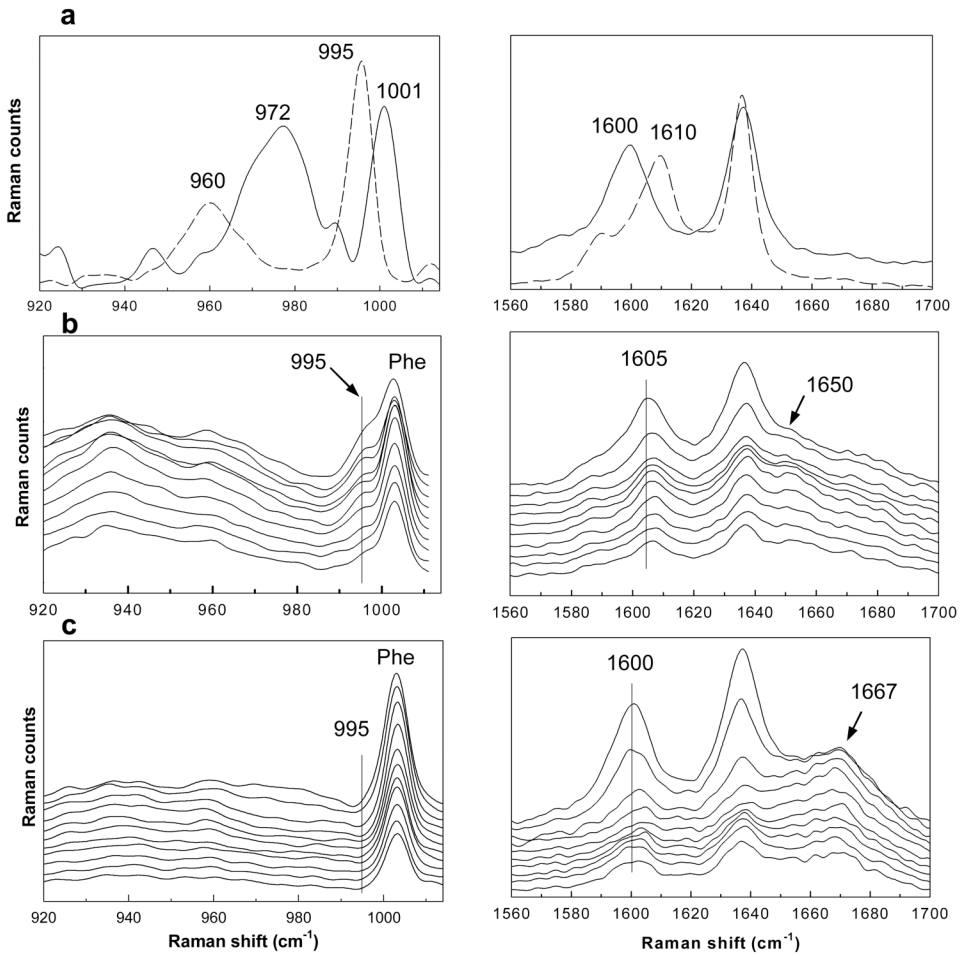

Fig. 3.

Raman spectra in the 920–1014 cm^{-1} and 1560–1700 cm^{-1} regions which are used to track the enzymatic dephosphorylation of R-P_3 in pigskin: (a) Raman spectra of resveratrol (-----) and R-P_3 (—) solutions (0.2 M), (b) confocal Raman spectra of pigskin following the application of an R-P_3 suspension (20h at 34°) from the surface of the SC (top spectrum) to a depth of ~60 μm in 3 μm increments, (c) confocal Raman spectra of pigskin exposed to steam prior to the application of R-P_3 presented as in (b). Several bands important in the analysis are highlighted (see text).

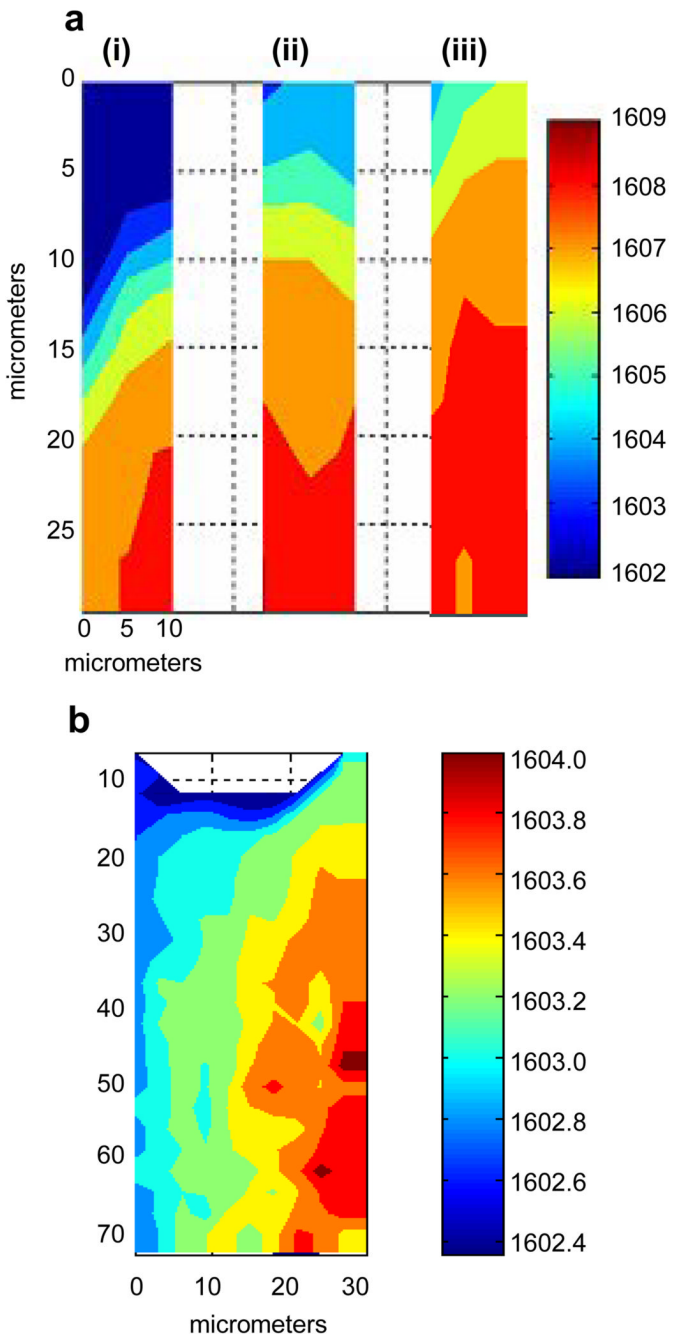

Fig. 4.

The time-dependence of R-P_3 dephosphorylation in the stratum corneum and viable epidermis as depicted by images of the frequency shift in the 1600–1610 cm^{-1} band: (a) encompassing the SC (top of image) and the boundary of viable epidermis (bottom) after the application of 0.2M R-P_3 to intact skin for 5h at 34°C, maps were acquired in the same area of 30μm (depth) × 10μm (width) at room temperature after treated skin was placed under Raman microscope for (i) 7h, (ii) 22h, (iii) 33h; (b) frequency images acquired after 0.2M R-P_3 was applied (20h at 34°C) to the viable epiderrmis of tape-stripped skin mapped over 75μm (depth in viable epidermis) × 30μm (width). The data collection took ~14h starting at the confocal line on the left side and ending at the 8^{th} confocal line on the right side. A linear baseline was applied to

the Raman spectra between 1575–1700 cm^{-1} prior to running the ISys Spectral Moments algorithm within the 1590–1620 cm^{-1} region to determine the position of the C=C stretching band using a conventional center of gravity calculation.

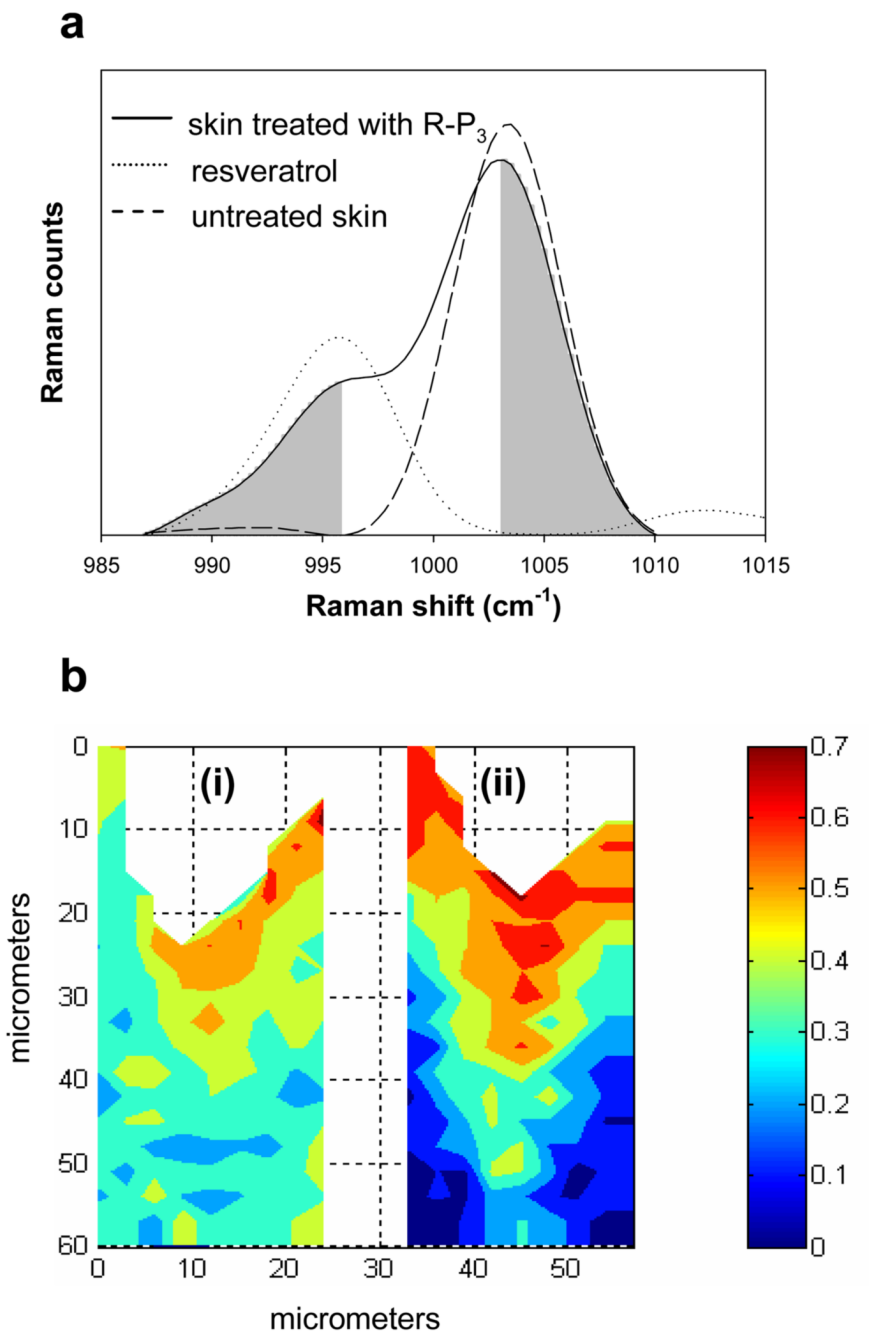

Fig. 5.

The determination of the spatial distribution of resveratrol in skin as measured by confocal Raman image planes. (a) The suitability of utilizing the band area ratio of the low frequency half of the 995 cm^{-1} band in resveratrol to the high frequency half of endogenous skin phe band (1004 cm^{-1}) (both shaded) to characterize the resveratrol concentration in skin. Both skin spectra were acquired at a depth of 8 μm beneath the skin surface. (b) The spatial distribution of resveratrol in skin depicted by confocal Raman image planes of the above described ratio after: (i) a resveratrol triphosphate suspension was applied to skin, and (ii) after a resveratrol suspension was applied to skin. The color bar shown on the right applies to both images. A

linear baseline between 985–1014 cm^{-1} was applied to the Raman spectra prior to band area integration.